Asian Journal of Pharmaceutical Sciences 13 (2018) 425–437

Available online at www.sciencedirect.com

ScienceDirect

journal homepage: www.elsevier.com/locate/AJPS

Original Research Paper

# Fabrication and characterization of spearmint oil loaded nanoemulsions as cytotoxic agents against oral cancer cell☆

*Sukannika Tubtimsri*[a,b], *Chutima Limmatvapirat*[c], *Siripan Limsirichaikul*[d], *Prasert Akkaramongkolporn*[b], *Yutaka Inoue*[e], *Sontaya Limmatvapirat*[b,*]

[a] *Faculty of Pharmaceutical Science, Burapha University, Thailand*
[b] *Department of Pharmaceutical Technology, Faculty of Pharmacy, Silpakorn University, 6 Rachamankra Road, Ampur Mueng, Nakhon Pathom 73000, Thailand*
[c] *Department of Pharmaceutical Chemistry, Faculty of Pharmacy, Silpakorn University, Thailand*
[d] *Department of Biopharmacy, Faculty of Pharmacy, Silpakorn University, Thailand*
[e] *Laboratory of Drug Safety Management, Faculty of Pharmacy and Pharmaceutical Science, Josai University, Japan*

ARTICLE INFO

*Article history:*
Received 6 November 2017
Revised 14 February 2018
Accepted 26 February 2018
Available online 16 March 2018

*Keywords:*
Nanoemulsions
Spearmint oil
Coconut oil
Surfactants
Anticancer
NMR

ABSTRACT

Spearmint oil (SMO), a commonly used essential oil for oral care products, possesses various interesting functions, especially for anticancer property. However, the application of SMO for cancer treatment is limited due to water insoluble. In the present study, nanoemulsions, which have been widely accepted as dosage forms for poorly water-soluble drugs, were selected as candidate carriers for SMO to inhibit oral cancer cell. The nanoemulsions were fabricated using phase inversion temperature method. The factors affecting formation and properties of nanoemulsions including type and amount of surfactants, oil loading and ratio of SMO to virgin coconut oil (VCO) were investigated. Among the surfactants used, the nanoemulsions containing polyoxyethylene castor oil derivatives (Kolliphor®EL; PCO35, Cremophor®RH40; PCO40, Eumulgin®CO60; PCO60) and polyoxyethylene sorbitan fatty acid esters (PSF80) showed 100% creaming after temperature cycling test indicating excellent physical stability while those containing PCO40 demonstrated more transparency and better physical stability. With an increasing amount of PCO40, the droplet size tended to decrease and was in the nano-size range (<1000 nm) after increasing to more than 5% (w/w). SMO-VCO loading also influenced on the droplet size. At 5% (w/w) PCO40, the maximum SMO-VCO loading of 25% (w/w) to attain nanoemulsions was observed. Moreover, the composition of oils had an impact on size of emulsions. The transparent nanoemulsions were only prepared in the range of SMO-VCO from 40:60 to 80:20, suggesting the optimum ratio of SMO to

☆ Peer review under responsibility of Shenyang Pharmaceutical University.

* Corresponding author. Department of Pharmaceutical Technology, Faculty of Pharmacy, Silpakorn University, 6 Rachamankra Road, Ampur Mueng, Nakhon Pathom 73000, Thailand. Tel.: +66-34-255800.
*E-mail address:* limmatvapirat_s@su.ac.th (S. Limmatvapirat).

https://doi.org/10.1016/j.ajps.2018.02.003

surfactant and the composition of oils were the critical factors for formation of nanoemulsions. NMR study disclosed that the interaction between PCO40 with both VCO and SMO should be a possible stabilization mechanism. Furthermore, the SMO-VCO nanoemulsions exhibited significant cytotoxic effect against oral carcinoma (KON) cell line using MTT assay. The finding, therefore, revealed the good feasibility of SMO-VCO nanoemulsions as novel carriers for treating of oral cancer.



## 1. Introduction

Head and neck cancers are regarded as the sixth most in cancer patients worldwide with approximately 700 000 new cases a year and 1.9% of all cancer deaths rate each year [1]. More than 90% of head and neck cancers are originated at the mucosal surfaces of oral cavity, oropharynx and larynx regions [2] while more than 65% of oral cancer cases are diagnosed and treated after progressing to advance stages [3]. The incident rate of new oral cancer case of male is nearly twice as female. The tobacco use, alcohol consumption, betel nut chewing, human papilloma virus infection, dentures wearing and poor oral hygiene are risk factors of oral cancer. Surgery, chemotherapy and radiation therapy are commonly used for oral cancer treatment. In general, chemotherapeutic agents should be the first choice drug for metastatic oral cancer treatment. Unfortunately, normal cells are affected, leading to systemic adverse effects and low patient acceptance. Moreover, chemotherapy is expensive and is also affected by cancer drug resistance. Early diagnosis or treatment using topical products that could eradicate newly formed cancer cells at the surface site might therefore be a better choice to avoid above mentioned disadvantages.

Spearmint oil (SMO), obtained from *Mentha spicata* leave, is one of the commonly used essential oils for oral care products. The main active components of SMO are terpene derivatives including carvone (70%) and limonene (15%) [4] which demonstrate various pharmacological properties [5,6] including anti-inflammatory, antispasmodic, antioxidant, antibacterial, antifungal, and antitumor activities. Regarding anticancer activity, SMO has been revealed for cytotoxicity against a variety of tumor cells including human mouth epidermal carcinoma, murine leukemia [7], human epithelial type 2 [8] and human breast adenocarcinoma cell line [9] so it might be a safe and potential cytotoxic agent for cancer treatment, especially for local therapeutic of oral cancer. Nevertheless, SMO shows a limited water solubility and inadequate biocompatibility in form of native oil and therefore need a water compatible carrier with high oil loading for targeting SMO to cancer cell.

Nanoemulsions are colloidal systems which are widely applied in diverse areas including drug delivery systems. They offer several advantages as good carriers for lipophilic drugs [10] such as high drug loading, kinetically stable, safe and promoting drug absorption. Additionally, the abilities of nanoemulsions to enhance permeability of cytotoxic drugs such as piplartine [11], carvone and isoniazid [12] into cancer cells including breast cancer, melanoma and colon cancer have been reported.

Formation of nanoemulsions has been successfully achieved by several fabrication technics including high and low energy method. The high energy method needs large mechanical force and energy for droplet size reduction while low energy method forms nanoemulsions through changing properties of system [13]. The high energy method demonstrates several good aspects in terms of easily formed nanoemulsions and scalability, however it still shows some disadvantages including cost of specialized equipment and generation of excessive heat that sometimes affects the stability of drugs. With regard to this concern, the phase inversion temperature (PIT) method which is one of low energy method, has been widely accepted for preparation of stable nanoemulsions [14]. Nevertheless, the formation and properties of corresponding nanoemulsions by this method have been largely influenced by the process and formulation parameters which need to be carefully elucidated in order to obtain the specific conditions for each active component [15].

Therefore, the purpose of this study was to evaluate the feasibility of nanoemulsions as carrier for targeting SMO to oral cancer cell. Parameters affecting the formation and physical properties of nanoemulsions through phase inversion method including type and amount of surfactants, oil loading, and ratio of SMO to virgin coconut oil (VCO) were investigated. Furthermore, the cytotoxic against a human oral squamous carcinoma cell line (KON) of optimal nanoemulsions was also elucidated.

## 2. Materials and methods

### 2.1. Materials

Spearmint oil (SMO, Lot NO.116BA290), Eumulgin®CO60 (PCO60, ANA NO.15090113) and Brij®72 (PAE2, ANA NO.16110005) were kind gifts from Greater Pharma, Thailand. Virgin coconut oil (VCO, Lot No. SS54/06177-01) was obtained from Tropicana oil, Thailand. Brij® 30 (PAE4, Lot NO.1/2157275), Cremophor® RH40 (PCO40, Lot NO.1640292400), Tween®20 (PSF20, Lot No. G190074), Tween®60 (PSF60, Lot No. G178174) and Tween®80 (PSF80, Lot NO. 1324202301081466) were purchased from P.C. drug center, Thailand. Cremophor®A25 (PAE25, Lot NO.5411-05) and Kolliphor® EL (PCO35, Lot NO.31163947G0) were received from BASF. The 3-(4, 5-dimethylthiazol-2-yl)-2, 5-diphenyltetrazolium bromide (MTT, Lot NO.39H5076) was purchased from SIGMA. Human

**Table 1 – Composition of each emulsion used in the study.**

| Factors studied | Surfactants* (%, w/w) | | | | | | | | | Oil (%, w/w) | | Water (%, w/w) |
|---|---|---|---|---|---|---|---|---|---|---|---|---|
| | PAE2 | PAE4 | PAE25 | PSF20 | PSF60 | PSF80 | PCO35 | PCO40 | PCO60 | SMO | VCO | |
| Type of surfactants | | | | | | | | | | | | |
| | 10.0 | – | – | – | – | – | – | – | – | 5.0 | 5.0 | 80.0 |
| | – | 10.0 | – | – | – | – | – | – | – | 5.0 | 5.0 | 80.0 |
| | – | – | 10.0 | – | – | – | – | – | – | 5.0 | 5.0 | 80.0 |
| | – | – | – | 10.0 | – | – | – | – | – | 5.0 | 5.0 | 80.0 |
| | – | – | – | – | 10.0 | – | – | – | – | 5.0 | 5.0 | 80.0 |
| | – | – | – | – | | 10.0 | – | – | – | 5.0 | 5.0 | 80.0 |
| | – | – | – | – | – | – | 10.0 | – | – | 5.0 | 5.0 | 80.0 |
| | – | – | – | – | – | – | – | 10.0 | – | 5.0 | 5.0 | 80.0 |
| | – | – | – | – | – | – | – | – | 10.0 | 5.0 | 5.0 | 80.0 |
| Amount of PCO40 | | | | | | | | | | | | |
| | – | – | – | – | – | – | – | 2.5 | – | 5.0 | 5.0 | 87.5 |
| | – | – | – | – | – | – | – | 5.0 | – | 5.0 | 5.0 | 85.0 |
| | – | – | – | – | – | – | – | 10.0 | – | 5.0 | 5.0 | 80.0 |
| | – | – | – | – | – | – | – | 20.0 | – | 5.0 | 5.0 | 70.0 |
| Amount of oil | | | | | | | | | | | | |
| | – | – | – | – | – | – | – | 5.0 | – | 2.5 | 2.5 | 90.0 |
| | – | – | – | – | – | – | – | 5.0 | – | 5.0 | 5.0 | 85.0 |
| | – | – | – | – | – | – | – | 5.0 | – | 7.5 | 7.5 | 80.0 |
| | – | – | – | – | – | – | – | 5.0 | – | 10.0 | 10.0 | 75.0 |
| | – | – | – | – | – | – | – | 5.0 | – | 12.5 | 12.5 | 70.0 |
| | – | – | – | – | – | – | – | 5.0 | – | 15.0 | 15.0 | 65.0 |
| | – | – | – | – | – | – | – | 5.0 | – | 17.5 | 17.5 | 60.0 |
| | – | – | – | – | – | – | – | 5.0 | – | 20.0 | 20.0 | 55.0 |
| Ratio of SMO:VCO | | | | | | | | | | | | |
| | – | – | – | – | – | – | – | 10.0 | – | 10.0 | – | 80.0 |
| | – | – | – | – | – | – | – | 10.0 | – | 9.0 | 1.0 | 80.0 |
| | – | – | – | – | – | – | – | 10.0 | – | 8.0 | 2.0 | 80.0 |
| | – | – | – | – | – | – | – | 10.0 | – | 7.0 | 3.0 | 80.0 |
| | – | – | – | – | – | – | – | 10.0 | – | 6.0 | 4.0 | 80.0 |
| | – | – | – | – | – | – | – | 10.0 | – | 5.0 | 5.0 | 80.0 |
| | – | – | – | – | – | – | – | 10.0 | – | 4.0 | 6.0 | 80.0 |
| | – | – | – | – | – | – | – | 10.0 | – | 3.0 | 7.0 | 80.0 |
| | – | – | – | – | – | – | – | 10.0 | – | 2.0 | 8.0 | 80.0 |
| | – | – | – | – | – | – | – | 10.0 | – | 1.0 | 9.0 | 80.0 |
| | – | – | – | – | – | – | – | 10.0 | – | – | 10.0 | 80.0 |

*Polyoxyethylene alkyl ethers (PAE): polyoxyl 2 stearyl ether (PAE2), polyoxyl 4 lauryl ether (PAE4), polyoxyl 25 cetostearyl ether (PAE25)
Polyoxyethylene sorbitan fatty acid esters (PSF): polyoxyethylene 20 sorbitan monolaurate (PSF20), polyoxyethylene 20 sorbitan monostearate (PSF60), polyoxyethylene 20 sorbitan monooleate (PSF80)
Polyoxyethylene caster oils (PCO): polyoxyl 35 castor oil (PCO35), polyoxyl 40 hydrogenated castor oil (PCO40), polyoxyl 60 hydrogenated castor oil (PCO60).

oral squamous cancer cell (KON, Lot NO.01262007) derived from metastatic site (cervical lymph node) was obtained from JCRB cell bank. All other chemicals were of reagent grade and used as received. The structures of investigated surfactants are presented in Fig. 1.

### 2.2. *Preparation of nanoemulsions*

The nanoemulsions containing SMO-VCO blended oils were prepared by phase inversion temperature method as previously described [16,17]. Briefly, an oil phase composed of predetermined weights of SMO, VCO and surfactant was mixed and heated to 62 °C. The oil phase was added into the water phase which was previously heated at 65 °C and then homogenized at 3800 rpm for 5 min using a homogenizer (IKA T25 digital, Staufen, Germany) and before cooling down to room temperature. The investigated factors for each emulsion are summarized in Table 1.

The obtained emulsions were then comparatively evaluated for their physical stability including the presence of creaming or cracking, droplet size and morphology. The optimized nanoemulsions were selected for further cytotoxicity test.

### 2.3. *Visual observation of cracking and creaming*

A 30 ml of each nanoemulsion was placed into a glass bottle with a screw cap (height 65 mm and 25 mm internal diameter), left standing at 25 ± 2 °C for 1 d and then observed for physical appearance. Cracking was referred as a permanent separation of dispersed phase indicated by the oil layer at the top of emulsions and denoted as physical instability. In case the emulsions were separated into cream and serum layers,

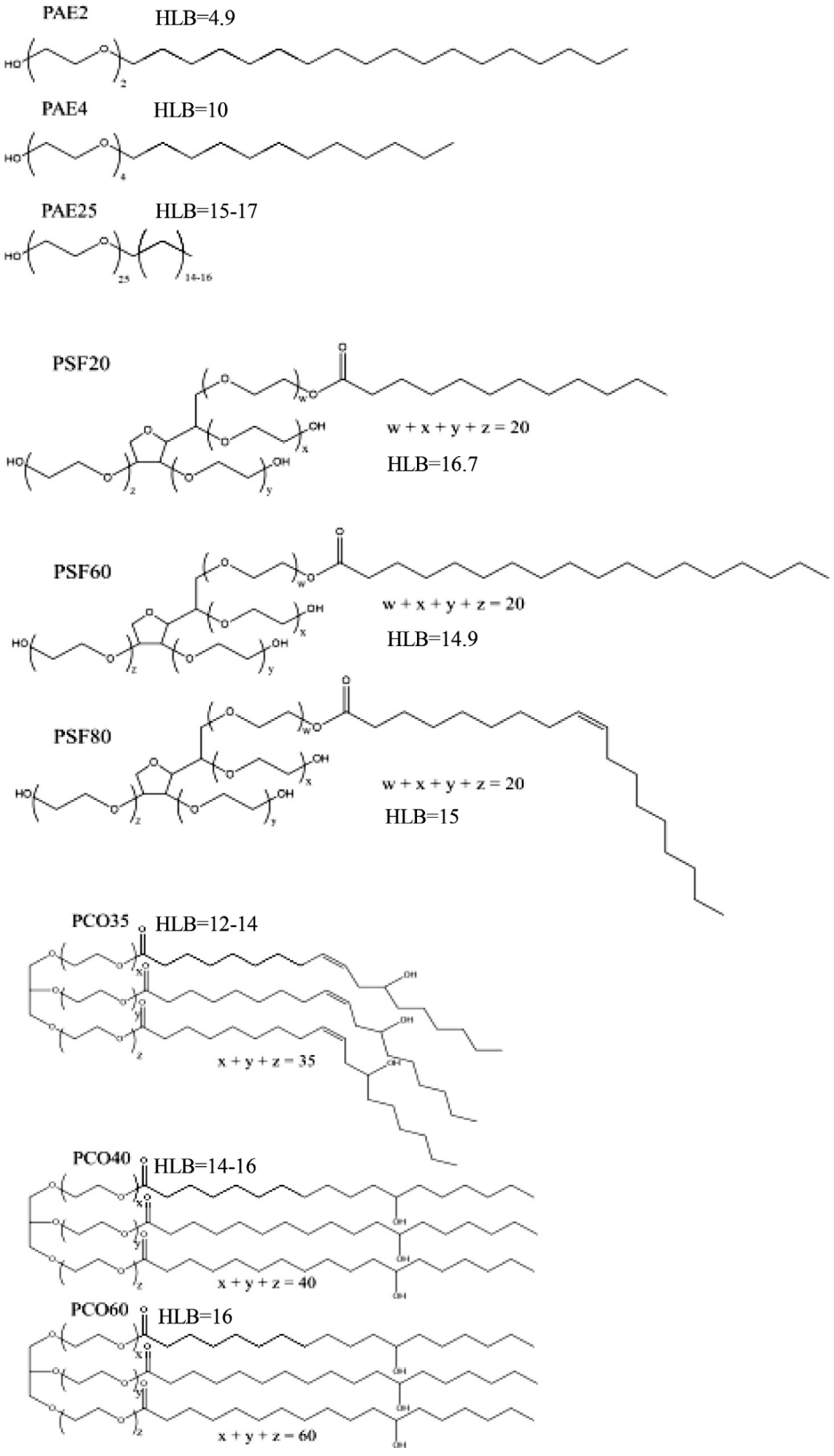


**Fig. 1 – Chemical structures of the surfactants in current study.**

the percent creaming was determined by measurement of the height of cream layer (top layer) and total height of emulsions [18] as expressed in Eq. (1).

$$\text{Creaming (\%)} = 100 \times \frac{\text{Height of cream layer}}{\text{Total height of emulsion}} \quad (1)$$

The temperature cycling test was also performed for all nanoemulsions to elucidate their physical stability. Each emulsion was alternatively kept at 4 °C for 24 h and 45 °C for 24 h. The temperature cycle was repeated for 6 times and then the samples were checked for physical appearance as compared to initial. All measurements were run in triplicate.

### 2.4. Droplet size determination

The droplet size of nanoemulsions was evaluated using either dynamic light scattering (Zetasizer Nano-ZS, Malvern Instruments, UK) or laser particle size analyzer (LA-950, Horiba, Japan). The nanoemulsions with the diameter of oil droplet size less than 100 nm were measured using Nano-ZS particle size analyzer while those of larger than 100 nm were evaluated by LA-950 particle size analyzer. Each sample was analyzed in triplicate.

### 2.5. Characterization of oil droplets

The morphology of internal phase of emulsions was characterized by either optical microscopy or atomic force microscopy (AFM). In case of emulsions with micron size droplets, the measurement was performed by optical microscope (CX41 RF, Olympus, Japan). Each sample was directly placed on the slide and visually observed through the digital eye piece (AM423X, ANMO Electronic, Taiwan). The AFM (Nanowizard III, JPK, Germany) was used for evaluation of emulsions with submicron size droplets, especially lower than 100 nm. All samples were diluted 10 times with deionized water. 3 µl of each diluted sample was dropped on a freshly cleaved mica disk and dried at room temperature in a fume hood. After 24 h, the dried samples were examined using the tapping mode by nano-probe cantilever tip (NSG11/TiN/20, NT-MDT, Russia). The images were scanned at 4 µm x 4 µm.

### 2.6. $^1H$-$^1H$ (NOESY) NMR spectroscopy

The nanoemulsions containing SMO-VCO blended oils were prepared by the same method as described in Section 2.2 but distilled water was substituted by deuterium oxide ($D_2O$) at the same volume. Other related substances including PCO40 were dissolved in $D_2O$. Nuclear magnetic resonance (NMR) spectroscopy analysis was performed using a Varian 700 MHz NMR spectrometer (Agilent Technologies Inc., USA) with an HCN probe operating at 699.7 MHz. The other measurement conditions were a mixing time of 0.15 sec, a pulse width of 90%, a relaxation delay of 1.0 sec, a scan time of 0.500 sec, and a temperature of 25 °C. All samples were measured under the same conditions.

### 2.7. Cytotoxicity test

The KON cell line was grown using a DMEM cell culture medium supplemented with 10% v/v fetal bovine serum (FBS) and 0.01% (v/v) L-glutamine solution. The cell suspensions were incubated at 37 °C in a 5% $CO_2$ incubator (KBF-240, Binder, Germany).

The anticancer properties of optimized nanoemulsions were evaluated by MTT assay. The KON cell line ($3 \times 10^4$ cell/well) was treated with each nanoemulsion containing different amounts of SMO in a 96 well culture plate for 24 h. Each emulsion was diluted with DMEM cell culture medium to 4, 2, 1%, 0.5%, 0.25%, 0.125%, 0.0625%(v/v) in each well (total volume in each well was 100 µl). The 20 µg/ml 5-FU solution was selected as a positive control. After incubation, the samples were removed and 50 µL of MTT solution was added to the culture plates (final concentration of MTT solution was 0.5 mg/ml). The plates were covered for light protection using aluminum foil and further incubated at 37 °C in 5% $CO_2$ for 3 h. The purple formazan of cell production was dissolved by adding 50 µl of DMSO to each well. The cell viability was monitored using absorbance at 570 nm (BP800, BIOHIT Plc, Finland). The data were recorded and analyzed for the mean values and the standard deviation. The percentage of cell viability was calculated by the following Eq. (2)

$$\text{Cell viability (\%)} = 100 \times \frac{\text{Mean absorbance of treated cell}}{\text{Mean absorbance of untreated cell}} \quad (2)$$

### 2.8. Cell morphology

The influence of nanoemulsions on KON cell lines was studied by a bright field microscopy. The cells were incubated with 0.34% (v/v) ($IC_{60}$) and 0.46% (v/v) ($IC_{80}$) of SMO-VCO (80:20) nanoemulsions for 24 h and then observed for morphological changes. The cells without treated and treated with 20 µg/mL 5-FU were used as negative control and positive control, respectively. The images were collected with 200x by a digital camera (DP22, Olympus, Japan).

Additionally, the influence of SMO-VCO nanoemulsions on nucleus fragmentation was determined by staining the cells with DAPI probes (4′, 6-diamidino-2-phenylindole, dihydrochloride). KON cells were treated with 0.34% (v/v) ($IC_{60}$) SMO-VCO (80:20) nanoemulsions for 24 h. A solution of 20 µg/mL 5-FU was used as the positive control. After washing with phosphate buffered saline (PBS), cells were fixed in 4% (v/v) paraformaldehyde for 10 min, permeabilized with 0.2% (v/v) Triton-X-100 and stained with 300 nM DAPI for 10 min in the dark cabinet. The resulting cells were rewashed with PBS and observed using an inverted fluorescent microscope (ECLIPSR Ts2, Nikon, Japan) with blue filters.

### 2.9. Statistical analysis

Statistical analysis was performed using the SPSS software version 10.0 for Windows (SPSS Inc., Chicago, IL, USA). The data were computed using one-way ANOVA analysis followed by Tukey's test at the 95% confidence level.

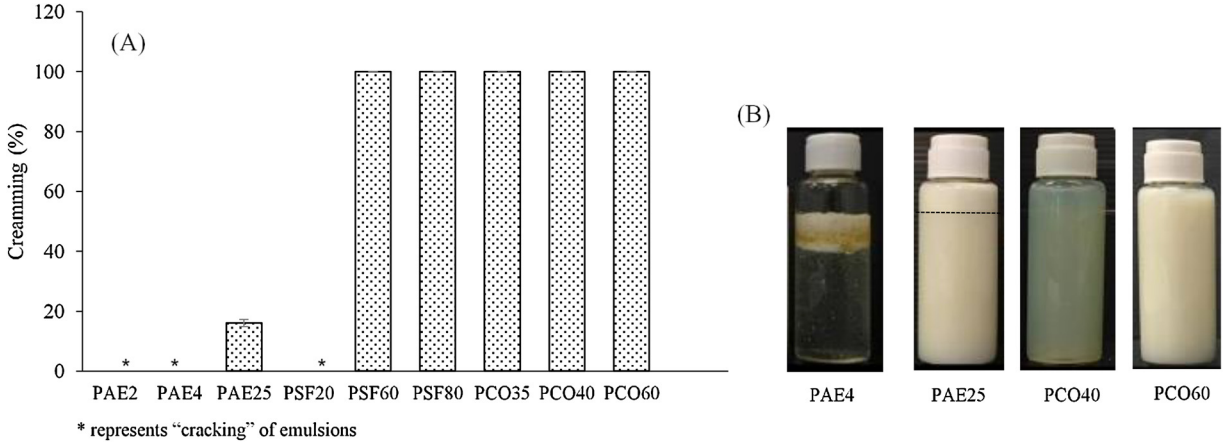


**Fig. 2 – Physical stability of SMO-VCO (50:50) nanoemulsions containing different surfactants as indicated by percent creaming (A) and appearance (B).**

## 3. Results and discussion

### 3.1. *Effect of type of surfactants on physical stability of SMO-VCO emulsions*

The formation of stable emulsions is dependent on the coverage of surfactants at the interfacial site of dispersed phase which is mainly influenced by the molecular structure of both surfactant and dispersed phase [19]. In case of O/W nanoemulsions, surfactants which have a relatively high hydrophilic–lipophilic balance (HLB) value are required for emulsion stabilization. Nevertheless, HLB alone is not a complete factor that could explain the stabilization process. The emulsions might show different properties such as physical appearance, size and size distribution although the surfactants which have relatively the same HLB values are used [20]. In this study, nonionic surfactants with different HLB values and molecular structure, i.e. polar head size, lipophilic chain length and configuration were selected from the groups of polyoxyethylene alkyl ethers, PAE (PAE2, PAE4, PAE25), polyoxyethylene sorbitan fatty acid esters, PSF (PSF20, PSF60, PSF80), and polyoxyethylene castor oils, PCO (PCO35, PCO40, PCO60) which are categorized in Generally Regarded as Safe (GRAS)[21]. The nanoemulsions with different surfactants were prepared and comparatively evaluated for their physical stability as shown in Figs. 2 and 3. The emulsions prepared from the PAE group showed physical instability as compared with other groups which were indicated by cracking (PAE2, PAE4) and lower percent creaming (PAE25) (Fig. 2). However, the stable emulsions with 100% creaming was observed in those containing PSF or PCO, except for emulsions containing PSF20. Additionally, the nanoemulsions containing PCO35 or PCO40 showed more optical transparency. The results suggested the influence of molecular structure of surfactants on formation and properties of nanoemulsions.

In order to further investigate the properties of nanoemulsions and their physical stability, the critical attribute i.e. droplet size was determined both before and after accelerated through temperature cycling. The droplet size of emulsions

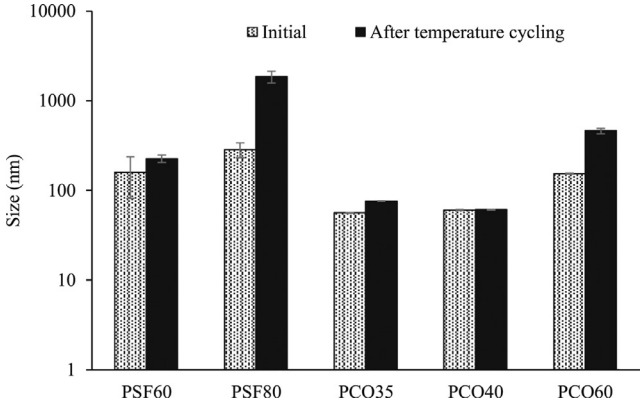


**Fig. 3 – Droplet size of SMO-VCO (50:50) nanoemulsions containing different surfactants before and after temperature cycling.**

containing PSF60, PSF80, PCO35, PCO40 and PCO60, which demonstrated 100% creaming, are illustrated in Fig. 3. The prepared nanoemulsions from PCO showed smaller droplet size than those fabricated from PSF. The droplet size of below 80 nm was observed when using PCO40 (60.1 ± 0.8 nm) and PCO35 (55.8 ± 0.2 nm) which were in accordance with the optical transparency. After temperature cycling, droplet size of all formulations, except those containing PCO40, showed a tendency to increase. The result was well correlated with previous reports [22,23], confirming the impact of molecular structure of surfactant on formation of nanoemulsions. Additionally, the finding revealed that PCO40 was the most suitable surfactant for emulsions composed of SMO-VCO as oil phase and therefore were selected for the rest of the study.

According to the physical stability described above, PAE which possesses a polar head of linear polyoxyethylene chain with less complexity demonstrated the least stable nanoemulsions as compared to those prepared from PSF or PCO which had a multiple and complex hydrophilic polyoxyethylene chains. Additionally, PAE25 which had the longest polyoxyethylene chain among the PAE groups could give more sta-

ble emulsions as compared to PAE2 and PAE4. The results implied that droplets of SMO-VCO blend oils needed relatively large polar hydrophilic head of surfactants to prevent them from coalescence [24].

The configuration of a hydrophobic chain also affected the formation and properties of SMO-VCO nanoemulsions. With the same polar head, nanoemulsions prepared from PSF80 or PSF60 with hydrophobic carbon chain length of 18 indicated more stability as compared to those prepared from PSF20 with carbon chain length of 12. Additionally, the bend structure of hydrophobic chain (PSF80) seemed to be not a good configuration for formation of nanoemulsions as compared to the straight chain (PSF60) [25,26]. This might be attributed to the shorter path of penetration into the oil droplets. The long straight chain as indicated in PSF60 should provide a longer path of penetration. It was also noted that the multiple hydrophobic chains as observed in all grades of PCO could facilitate the formation of nanoemulsions. Therefore, it might be reasonable to conclude that the long, straight and multiple chain of surfactants could assist the adsorption into the interface of oil droplets and help stabilization of SMO-VCO nanoemulsions.

### 3.2. *Effect of amount of PCO40 on droplet size of SMO-VCO emulsions*

One of key parameters for fabrication of stable emulsions is the amount of surfactant. The surfactant should be sufficient to provide protection of oil droplets against coalescence [27]. In order to evaluate the influence of PCO40 concentration on the droplet size, the SMO-VCO (50:50) blend oils with a fixed total amount of 10% (w/w) were prepared at the concentration range of PCO40 from 2.5% to 20% (w/w) as shown in Fig. 4A. With an increasing of PCO40 concentration, the droplet size was dramatically reduced at the initial amounts from 2.5% to 5.0% (w/w) and approached the plateau at the concentration from 10% (w/w). The smallest droplet size of $55.8 \pm 2.4$ nm was obtained from the system using 20% (w/w) of PCO40. The results were in good accordance with the formation of D-limonene based nanoemulsions as described by Zahi et al. [28].

Generally, the ultimate size of oil droplets is dependent on the balance of 2 concomitant and opposing processes, i.e. droplet break up and coalescence. Droplet will break up by the shearing force while the coalescence can occur spontaneously which is due to the increased interfacial tension if the surface of oil droplets are not well protected. The final droplet radius ($r$) could be well explained by the Taylor's equation. $r \sim \gamma/(\eta_c \dot{\gamma})$, where $\gamma$ is the interfacial tension, $\eta_c$ is the continuous phase viscosity and $\dot{\gamma}$ is the shear rate [13]. In this case, the increased amount of PCO40 at the boundary of oil to water interface should be a possible explanation of reduced interfacial tension and generation of small droplets. Additionally, the absorption of surfactants at the oil surface should provide the steric hindrance due to the hydrophilic heads of PCO40 as described in Section 3.1. It should be also noted the required amount of surfactant for formation of nanoemulsions in this study was very low (5%, w/w) as compared with other reports [29–31]. The results suggested that another factor including the nature of oil phase might also have an influence on the formation of SMO-VCO nanoemulsions.

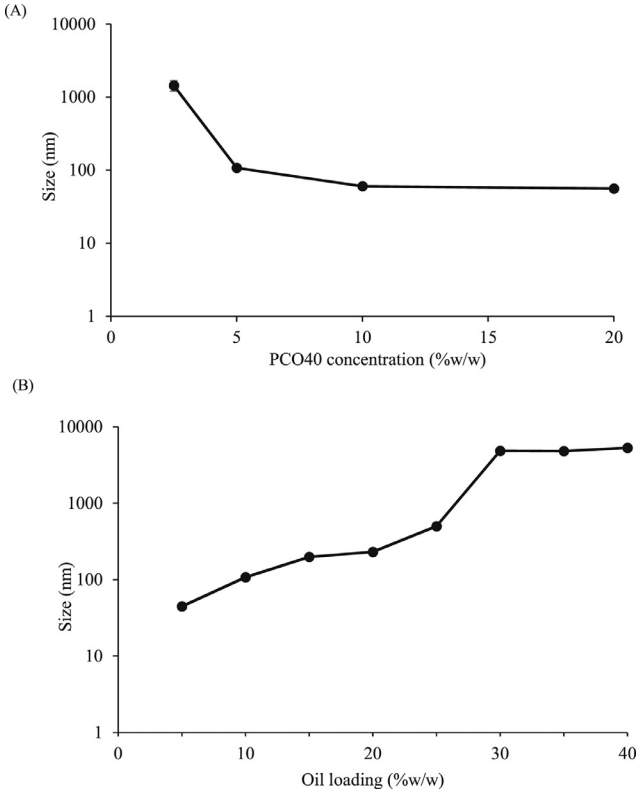


**Fig. 4 – Influence of (A) PCO40 concentration and (B) oil loading on droplet size of SMO-VCO nanoemulsions.**

### 3.3. *Effect of oil loading on droplet size of SMO-VCO emulsions*

The influence of percent of oil phase on the droplet size was further investigated by preparing a series of emulsions containing SMO-VCO (50:50) with a fixed amount of 5% w/w PCO40 and varied oil loading between 5% and 40% w/w. As illustrated in Fig. 4B, the droplet size was significantly increased as increase of percent oil loading. The droplet size of emulsion exceeded the nano scale (>1000 nm) as increasing percent of oil above 25% (w/w). This finding was well corresponded with those observed in the influence of amount of surfactants and related reports [32], revealing that the optimum ratio of oil to surfactant was also a critical factor for formation of nanoemulsions.

The increment of droplet size might be explained by the similar reasons as described in Section 3.2. As increasing the oil loading, the amount of the limited surfactant should not be enough to completely cover the oil droplet and prevent the re-coalescence during processing.

### 3.4. *Morphology of nanoemulsions*

The photomicrographs as observed through an optical microscope of SMO-VCO emulsions containing 20%–30% (w/w) oils are illustrated in Fig. 5A. The large globular droplets having

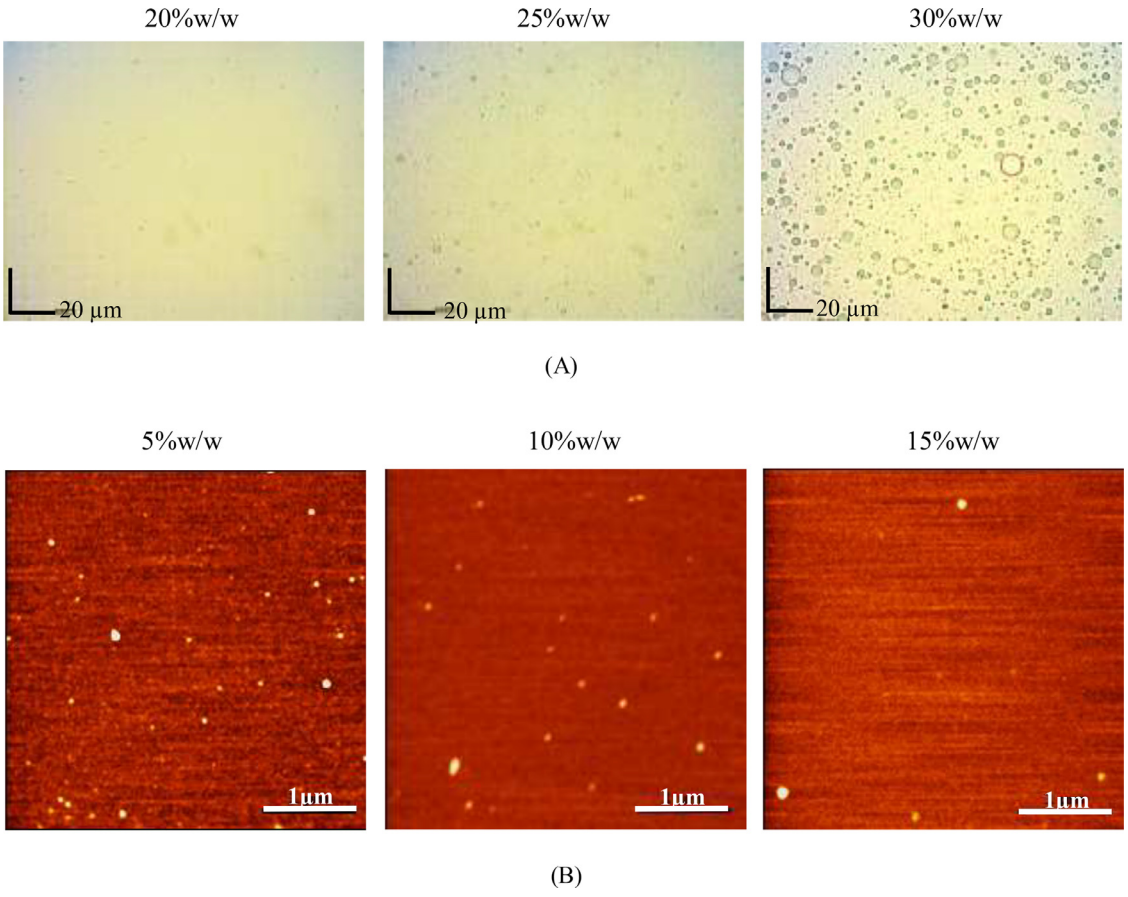


**Fig. 5 – (A) Optical microscopic images of SMO-VCO (50:50) nanoemulsions containing 20%, 25% and 30% (w/w) oils, (B) AFM images of SMO-VCO (50:50) nanoemulsions containing 5%, 10% and 15% (w/w) oils.**

the similar size with those measured by laser light scattering were clearly observed in the emulsions containing 30% (w/w) oil. The droplet size had a tendency to decrease as decreasing oil loading although the droplets were not obviously seen, especially for emulsions containing oil less than 25% (w/w). The result suggested a limit of optical microscopy for characterization of fast Brownian movement of sub-micron size oil droplets. In this study, AFM was selected as an alternative tool for the characterization of morphology of oil droplets in the submicron range. The AFM images of SMO-VCO nanoemulsions with different oil loading between 5% and 15% (w/w) are illustrated in the Fig. 5B. Similarly as observed by optical microscopy, the round oil droplets with a decrease in size were observed as decreasing the percent oil loading. Additionally, the size of droplets was well correlated with those measurements by particle size analyzers. The result confirmed that the droplets were spherical shape even downsizing to less than 100 nm.

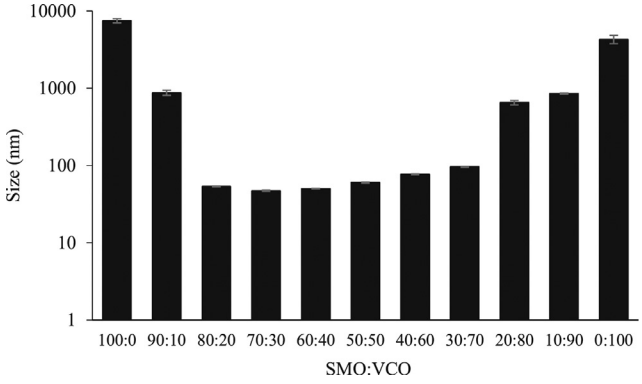


**Fig. 6 – Influence of SMO-VCO ratios on droplet size of nanoemulsions containing 10% w/w PCO40 and 10% (w/w) oil loading.**

### 3.5. *Effect of oil phase composition on droplet size of SMO-VCO emulsions*

According to the result described in Section 3.2, the formation of SMO-VCO (50:50) nanoemulsions easily occurred at the uncommon low level of surfactant which implied that the oil phase, especially ratio of SMO to VCO, might also affect the properties of corresponding emulsions. In order to elucidate this factor, the emulsions with different SMO-VCO ratios were prepared and comparatively evaluated for their droplet size as presented in Fig. 6. The systems containing only VCO (SMO-VCO 0:100) or only SMO (SMO-VCO 100:0) showed

milky emulsions with the droplet size of 4.3 and 7.5 μm, respectively. However, the emulsions with SMO-VCO at the ratio from 40:60 to 80:20 showed transparent nanoemulsions with nano scale droplet size (50–70 nm). The results demonstrated that oil phase composition (SMO-VCO ratio) played an important role for the formation of nanoemulsions, especially at low amount of surfactant. Our finding was supported by several studies. Chang and McClements reported that orange oil alone could not produce stable emulsions while the transparent nanoemulsions were only formed if 30%–50% w/w orange oil were blended with medium chain triglyceride [33]. Similar results were also observed with other volatile oils including pine oil [32], peppermint oil [34], and thyme oil [35].

Ostwald ripening is widely accepted as a major destabilizing mechanism of nanoemulsions. This phenomenon relates with the growth of oil droplets through the continuous phase in which the ripening rate could be explained by the following equation [36,37].

$$r^3 - r_0^3 = \omega t = \frac{4}{9}\alpha c D t \quad (4)$$

where $r$ is the mean droplet size, $\omega$ is the Ostwald ripening rate, $c$ is the solubility of the oil in the aqueous phase, and $D$ is the diffusion coefficient of the oil through the aqueous phase. $\alpha = 2\gamma V_m/RT$ ($\gamma$ is the interfacial tension, $V_m$ is the molar volume of the oil, $R$ is the gas constant, and $T$ is the absolute temperature). Consequently, the Ostwald ripening is mainly driven by $V_m$ and $c$ especially when diffusion coefficient, governed by the viscosity of dispersed phase, is comparatively unchanged.

With regard to the chemical structure of oil phase, the carvone, major component found in SMO [38], is a small non-polar molecule (MW = 150) as compared to trilaurin (MW = 639) which is the main triglyceride of VCO [39]. The calculated value of XLOGP3-AA (computation of octanol-water partition coefficients) of carvone and trilaurin was 2.4 and 15.4, respectively [40,41]. The $V_m$ and $c$ of SMO was therefore expected to be higher as compared to those of VCO and these might be a reasonable explanation for the faster Ostwald ripening rate and larger droplet size of emulsions containing pure SMO as compared to those containing only VCO. With an increase fraction of VCO from 10% to 50% of total oil, the droplet size was decreased from 888 nm to 47 nm, disclosing the ability of VCO to retard Ostwald ripening. The results might be explained by the influence of entropy of mixing that could be opposed to the droplet growth as previously described in earlier reports [36,42]. Considering the O/W emulsions comprising lipids with different water solubility, the molecules of higher water solubility oil (SMO) could more easily diffuse from the small droplets to larger droplets due to Ostwald ripening. Accordingly, the fraction of SMO in the larger droplets would be increased. The difference of oil composition among droplets of various sizes was thermodynamically unfavorable because of entropy of mixing. As a result, there was a thermodynamic force that drove in the opposite direction of Ostwald ripening effect.

Nonetheless, the prevention of Ostwald ripening as described above could not completely explain the phenomena observed in the emulsions, especially after incorporation of VCO more than 50%. The droplet size still had a tendency to increase as increasing VCO fractions. The mechanism related to this finding was still unclear. The possible explanation might be related to specific compatibility between the surfactants and oil phases which need to be further investigated.

### 3.6. *Investigation of interaction by NOESY NMR measurements*

NMR spectroscopy is commonly applied for structure elucidation as well as intra- and intermolecular interactions. For the interaction, several technics including a 2D-NOESY which provides information on two non-bonded protons that are within 5 Å in space [43] have been employed as a tool for studying the interaction among molecules. In this study, 2D NOESY was also used to investigate the interactions between PCO40 with SMO-VCO blended oils.

The $^1$H-$^1$H NOESY spectrum of each component in the SMO-VCO (50:50) nanoemulsions is illustrated in Fig. 7. The signal assignments along with the chemical structures of main compounds in VCO (trilaurin), and PCO40 are indicated with the capital letters and small caps, respectively while those for SMO (carvone and limonene) are shown by the integer numbers. Trilaurin showed the characteristic chemical shifts at about 4.0 ppm (A, C), 5.0 ppm (B), 2.0–2.2 ppm (D) and 1.0–1.5 ppm (G) which attributed to the methylene protons and methine protons of lauric acid side chains. PCO40 demonstrated signals of methylene protons of the hydrophobic hydrogenated ricinoleic side chain at chemical shifts around 1.0–1.5 ppm (c, e) and signals of oxymethylene protons of the hydrophilic polyoxyethylene chain at 3.5 ppm (g, h). SMO showed complicated NMR spectrum because it consisted of at least two major components including carvone and limonene. The $^1$H signals of carvone and limonene are assigned by integer numbers with green and blue colors, respectively. As obviously shown by a number of cross peaks in 2D-NMR, the interaction among the functional groups of PCO40, VCO and SMO was revealed. For examples, cross peaks were observed between $f_1$ (g, h) peaks of PCO40 with $f_2$ (A, C), $f_2$ (D) and $f_2$ (G) of VCO (as indicated by $\alpha_1$, $\alpha_2$ and $\alpha_3$, respectively). Additionally, the disappearance of cross peak of $f_1$ (g, h) and $f_2$ (B) was indicated. The results suggested the interaction between PCO40 and VCO. The interaction between PCO40 and SMO was also detected. The cross peaks between $f_1$ (c, e) of PCO40 and $f_2$ (2′) of limonene and those between $f_1$ (g, h) of PCO40 and $f_2$ (2) of carvone were discovered (as indicated by the $\beta_1$ and $\beta_2$).

With regard to the result of NMR, it might be reasonable to conclude that the PCO40 should be strongly absorbed at the interface of oil droplets by the interaction between PCO40 with both VCO and SMO. Consequently, the surfactant layer of PCO40 should completely cover the surface of the oil droplets and thus prevent from coalescence, resulting in the stabilization of nanoemulsions.

### 3.7. *Cytotoxic activities against oral cancer cell of SMO-VCO emulsions*

In order to study the feasibility of nanoemulsions as cytotoxic carriers for targeting oil to the oral cancer cells, the percent cell viability of KON cell line after being exposed to na-

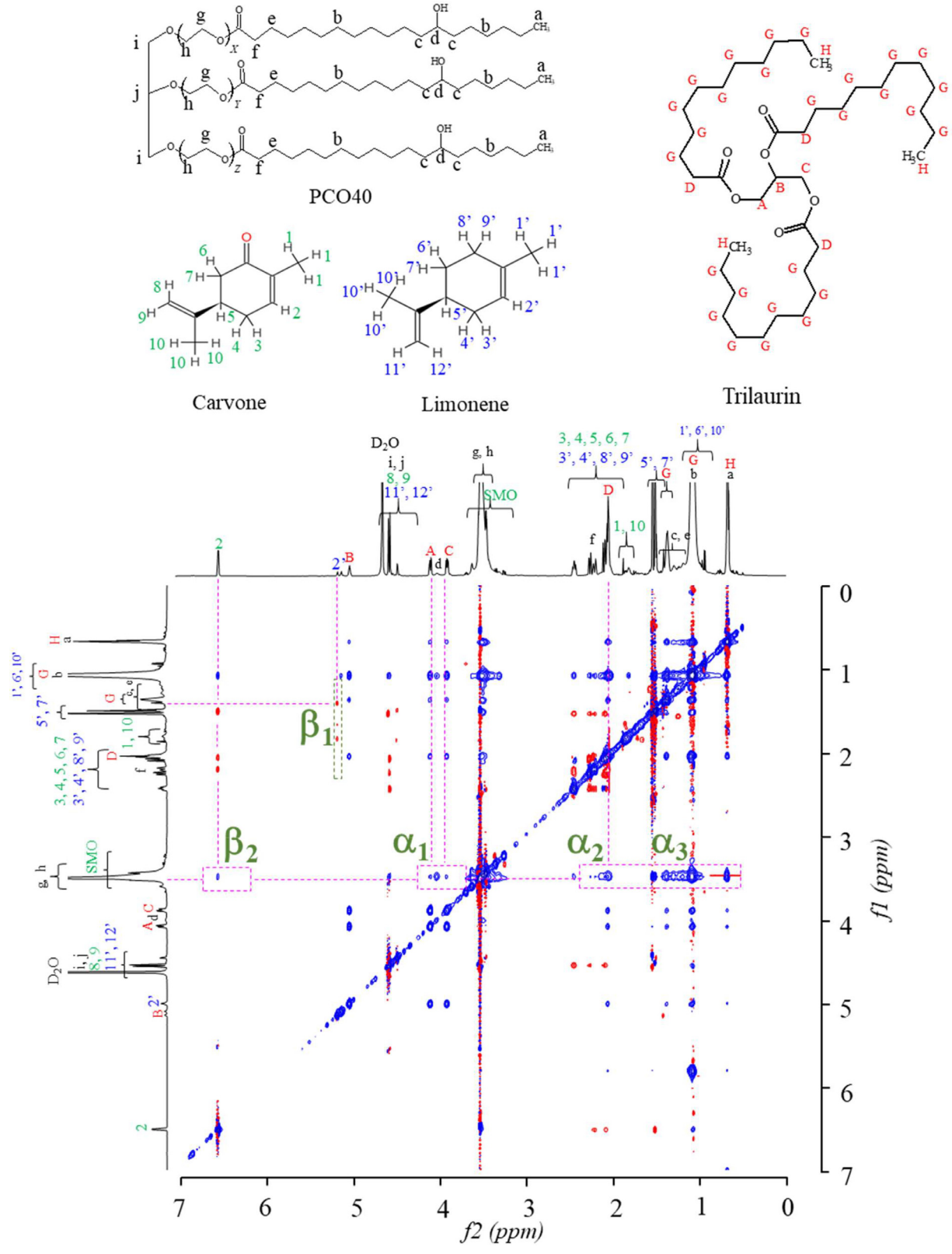


**Fig. 7 – $^{1}$H-$^{1}$H NOESY spectrum of SMO-VCO (50:50) nanoemulsion.**

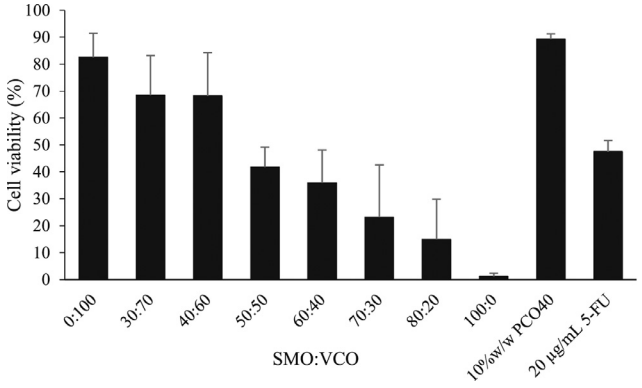


**Fig. 8 – Viability of KON cell after treated with 0.5%(v/v) nanoemulsions with different SMO-VCO ratios, 0.5% (v/v) of 10% (w/w) PCO40 solutions (negative control) and 20 µg/ml 5-FU (positive control).**

noemulsions containing various ratios of SMO-VCO and control samples was comparatively evaluated as shown in Fig. 8. The PCO40 solution (containing the same amount of surfactants as found in emulsions) did not clearly affect the cell viability while the percent cell viability was decreased to less than 50% after treated with a positive control sample (5-FU solutions). For emulsions containing only VCO (SMO-VCO 0:100), the percent cell viability was not clearly different from that treated with PCO40 solution (negative control) while it significantly decreased as increasing the SMO fraction in oil phase, suggesting the good feasibility of nanoemulsions as carriers for targeting SMO to destroy oral cancer cell. Additionally, the findings revealed the dose dependent relationship between amount of SMO and cytotoxic effect regardless of droplet size. Nevertheless, the SMO-VCO (100:0) emulsions were unstable. Therefore, SMO-VCO (80:20) nanoemulsions which contained maximum SMO loading and demonstrated good physical stability were therefore selected for further studies.

The influence of SMO-VCO (80:20) nanoemulsions on cell morphology was elucidated to confirm the cytotoxic effect and the mechanism of cell death as shown in Fig. 9. The KON cells were treated with nanoemulsions at the concentration which did not completely kill the cells, *i.e.* at the levels of $IC_{60}$ and $IC_{80}$ and then comparatively observed for their morphological change. As presented in Fig. 9A, the untreated group demonstrated healthy cells with good attachment to the well surface as indicated by good spreading and flattened morphology. However, after treated with SMO-VCO nanoemulsions, the loss of cell adhesion and cell shrinkage was clearly observed. Similar result was also clearly indicated in the cells treated with 5-FU. The result confirmed the cytotoxic effect of SMO-VCO nanoemulsions. Besides, the mechanism of cell death, which related with the nucleus fragmentation, was also investi-

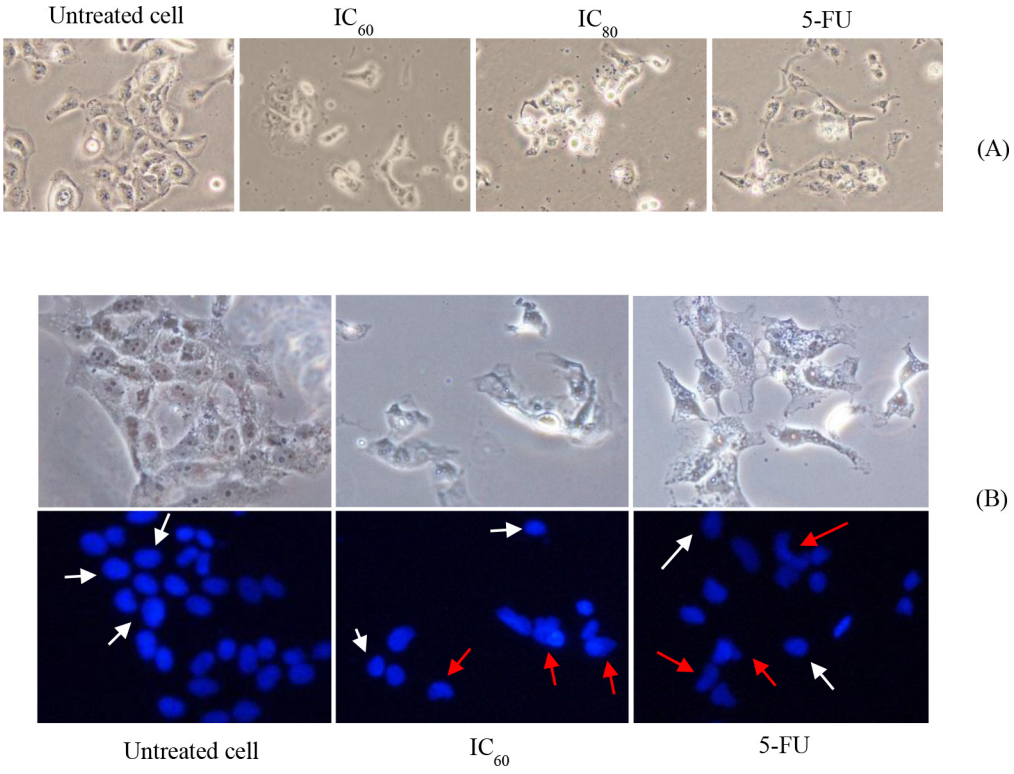


**Fig. 9 – (A) Bright field microscopic images of KON cancer cells after treated with control, SMO-VCO (80:20) at IC60 concentration, SMO-VCO (80:20) at $IC_{80}$ concentration, and 20 µg/ml 5-FU, (B) Fluorescent images of KON cancer cells after treated with control, SMO-VCO (80:20) at IC60 concentration, SMO-VCO (80:20) at $IC_{80}$ concentration, and 20 µg/ml 5-FU; White and red arrows show normal nucleus and nucleus fragmentation, respectively.**

gated by staining with DAPI probes as indicated by the fluorescent images in Fig. 9B. The nucleus fragmentation was clearly found in KON cells after exposure to either SMO-VCO (80:20) nanoemulsions or 5-FU solution. The result implied that the mechanism of cell death might be related with apoptosis. However, another supportive technic still need to be employed for further evaluation of the exact mechanism.

## 4. Conclusions

The SMO-VCO nanoemulsions with cytotoxic activity against oral cancer cell were successfully fabricated in this study. The finding disclosed the critical factors affecting the formation of stable nanoemulsions including type of surfactants, oil loading and SMO-VCO ratios. The most suitable surfactant for encapsulation of SMO-VCO blended oils was PCO40 which provided the most stable nanoemulsion. The SMO-VCO ratios which indicated the transparent nanoemulsion with droplet size less than 80 nm were in the limited range from 40:60 to 80:20. Additionally, the selected SMO-VCO nanoemulsions (80:20) demonstrated the cytotoxic effect against KON cells in which the mechanism might be the apoptosis. Therefore, the study revealed the good feasibility of SMO-VCO nanoemulsions as novel carriers for treatment of oral cancer.

## Conflict of interest

The authors declare that there are no conflicts of interest.

## Acknowledgments

The authors acknowledge the financial support received from Silpakorn University Research and Development Institute. The study was also supported by Faculty of Pharmacy, Silpakorn University. Our special thanks are extended to Mr. Toshinari Ezawa and Miss Rina Suzuki for their technical supports regarding NMR measurements.

REFERENCES

[1] Farquhar DR, Divaris K, Mazul AL, et al. Poor oral health affects survival in head and neck cancer. Oral Oncol 2017;73(Supplement C):111–17.
[2] Ali J, Sabiha B, Jan HU, Haider SA, Khan AA, Ali SS. Genetic etiology of oral cancer. Oral Oncol 2017;70:23–8.
[3] Vigneswaran N, Williams MD. Epidemiologic trends in head and neck cancer and aids in diagnosis. Oral Maxillofac Surg Clin North Am 2014;26(2):123–41 4.
[4] Kokkini S, Karousou R, Lanaras T. Essential oils of spearmint (Carvone-rich) plants from the island of Crete (Greece). Biochem Syst Ecol 1995;23(4):425–30.
[5] Wangjit K, Limmatvapirat C, Nattapulwat N, Sutananta W, Limmatvapirat S. Factors affecting formation of nanoemulsions containing modified coconut oil and spearmint oil. Asian J Pharm 2016;11(1):227–8.
[6] Ulbricht C, Costa D, M Grimes Serrano J, et al. An evidence-based systematic review of spearmint by the natural standard research collaboration. J Diet Suppl 2010;7(2):179–215 7.
[7] Manosroi J, Dhumtanom P, Manosroi A. Anti-proliferative activity of essential oil extracted from Thai medicinal plants on KB and P388 cell lines. Cancer Lett 2006;235(1):114–20 8.
[8] Stammati A, Bonsi P, Zucco F, Moezelaar R, Alakomi HL, von Wright A. Toxicity of selected plant volatiles in microbial and mammalian short-term assays. Food Chem Toxicol 1999;37(8):813–23.
[9] Jaafari A, Tilaoui M, Mouse HA, et al. Comparative study of the antitumor effect of natural monoterpenes: relationship to cell cycle analysis. Rev Bras Farmacogn 2012;22:534–40.
[10] Khanum R, Thevanayagam H. Lipid peroxidation: its effects on the formulation and use of pharmaceutical emulsions. Asian J Pharm 2017;12(5):401–11.
[11] Fofaria NM, Qhattal HSS, Liu X, Srivastava SK. Nanoemulsion formulations for anti-cancer agent piplartine—Characterization, toxicological, pharmacokinetics and efficacy studies. Int J Pharm 2016;498(1–2):12–22.
[12] Bhat MA, Iqbal M, Al-Dhfyan A, Shakeel F. Carvone schiff base of isoniazid as a novel antitumor agent: Nanoemulsion development and pharmacokinetic evaluation. J Mol Liq 2015;203(Supplement C):111–19.
[13] Singh Y, Meher JG, Raval K, et al. Nanoemulsion: concepts, development and applications in drug delivery. J Control Release 2017;252:28–49.
[14] Arshakyan GA, Zadymova NM. The effect of a lipophilic drug, felodipine, on the formation of nanoemulsions upon phase inversion induced by temperature variation. Colloid J 2017;79(1):1–12.
[15] Ostertag F, Weiss J, McClements DJ. Low-energy formation of edible nanoemulsions: Factors influencing droplet size produced by emulsion phase inversion. J Colloid Interface Sci 2012;388(1):95–102.
[16] Pengon S, Limmatvapirat C, Limmatvapirat S. Design of nanoemulsions through combination of fixed-volatile oils. Key Eng Mater 2011;486:123–6.
[17] Fernandez P, André V, Rieger J, Kühnle A. Nano-emulsion formation by emulsion phase inversion. Colloids Surf A: Physicochem Eng Aspects 2004;251(1):53–8.
[18] Prabhakar K, Afzal SM, Kumar PU, Rajanna A, Kishan V. Brain delivery of transferrin coupled indinavir submicron lipid emulsions—Pharmacokinetics and tissue distribution. Colloids Surf B 2011;86(2):305–13.
[19] Wooster TJ, Golding M, Sanguansri P. Impact of oil type on nanoemulsion formation and Ostwald ripening stability. Langmuir 2008;24(22):12758–65.
[20] Zafeiri I, Horridge C, Tripodi E, Spyropoulos F. Emulsions co-stabilised by edible pickering particles and surfactants: the effect of HLB value. Colloid Interface Sci 2017;17(Supplement C):5–9.
[21] Hauss DJ. Oral lipid-based formulations. Adv Drug Delivery Rev 2007;59(7):667–76.
[22] Dai L, Li W, Hou X. Effect of the molecular structure of mixed nonionic surfactants on the temperature of miniemulsion formation. Colloids Surf A: Physicochem Eng Aspects 1997;125(1):27–32.
[23] Weerapol Y, Limmatvapirat S, Nunthanid J, Sriamornsak P. Self-Nanoemulsifying drug delivery system of Nifedipine: Impact of hydrophilic–lipophilic balance and molecular structure of mixed surfactants. AAPS PharmSciTech 2014;15(2):456–64.
[24] Helgeson ME. Colloidal behavior of nanoemulsions: interactions, structure, and rheology. Curr Opin Colloid Interface Sci 2016;25(Supplement C):39–50.
[25] Zeng L, Xin X, Zhang Y. Development and characterization of promising Cremophor EL-stabilized o/w nanoemulsions containing short-chain alcohols as a cosurfactant. RSC Adv 2017;7(32):19815–27.

[26] Sanatkaran N, Masalova I, Malkin A. Effect of surfactant on interfacial film and stability of highly concentrated emulsions stabilized by various binary surfactant mixtures. Colloids Surf A 2014;461:85–91.
[27] Walker RM, Decker EA, McClements DJ. Physical and oxidative stability of fish oil nanoemulsions produced by spontaneous emulsification: effect of surfactant concentration and particle size. J Food Eng 2015;164(Supplement C):10–20.
[28] Zahi MR, Liang H, Yuan Q. Improving the antimicrobial activity of D-limonene using a novel organogel-based nanoemulsion. Food Control 2015;50(Supplement C):554–9.
[29] de Menezes Furtado C, de Faria FSEDV, Azevedo RB, et al. Tectona grandis leaf extract, free and associated with nanoemulsions, as a possible photosensitizer of mouse melanoma B16 cell. J Photochem Photobiol 2017;167(Supplement C):242–8.
[30] Zhang Y, Shang Z, Gao C, et al. Nanoemulsion for solubilization, stabilization, and in vitro release of pterostilbene for oral delivery. AAPS PharmSciTech 2014;15(4):1000–8.
[31] Pangeni R, Kang S-W, Oak M, Park EY, Park JW. Oral delivery of quercetin in oil-in-water nanoemulsion: In vitro characterization and in vivo anti-obesity efficacy in mice. J Funct Foods 2017;38(Part A):571–81.
[32] Pukale DD, Bansode AS, Pinjari DV, Sayed U, Kulkarni RR. Development of nanoemulsion of silicone oil and pine oil using binary surfactant system for textile finishing. J Surf Deterg 2017;20(5):1061–73.
[33] Chang Y, McClements DJ. Optimization of orange oil nanoemulsion formation by isothermal low-energy methods: Influence of the oil phase, surfactant, and temperature. J Agric Food Chem 2014;62(10):2306–12.
[34] Liang R, Xu S, Shoemaker CF, Li Y, Zhong F, Huang Q. Physical and antimicrobial properties of peppermint oil nanoemulsions. J Agric Food Chem 2012;60(30):7548–55.
[35] Ziani K, Chang Y, McLandsborough L, McClements DJ. Influence of surfactant charge on antimicrobial efficacy of surfactant-stabilized thyme oil nanoemulsions. J Agric Food Chem 2011;59(11):6247–55.
[36] Li Y, Le Maux S, Xiao H, McClements DJ. Emulsion-based delivery systems for tributyrin, a potential colon cancer preventative agent. J Agric Food Chem 2009;57(19):9243–9.
[37] Taylor P. Ostwald ripening in emulsions. Adv Colloid Interface Sci 1998;75:107–63.
[38] Ludwiczuk A, Skalicka-Woźniak K, Georgiev MI. Chapter 11—Terpenoids. In: Badal S, Delgoda R, editors. Pharmacognosy. Boston: Academic Press; 2017. p. 233–66.
[39] Debmandal M, Mandal S. Coconut (*Cocos nucifera* L.: Arecaceae): in health promotion and disease prevention. Asian Pac J Trop Med 2011;4(3):241–7.
[40] Information NCfB. PubChem Compound Database; CID=439570 Available from: https://pubchem.ncbi.nlm.nih.gov/compound/439570.
[41] Information NCfB. PubChem Compound Database; CID=10851 Available from: https://pubchem.ncbi.nlm.nih.gov/compound/10851.
[42] Kabal'nov AS, Pertzov AV, Shchukin ED. Ostwald ripening in two-component disperse phase systems: application to emulsion stability. Colloids Surf 1987;24(1):19–32.
[43] Khodov IA, Nikiforov MY, Alper GA, et al. Spatial structure of felodipine dissolved in DMSO by 1D NOE and 2D NOESY NMR spectroscopy. J Mol Struct 2013;1035(Supplement C):358–62.